0026-895X/09/7503-502–513$20.00
MOLECULAR PHARMACOLOGY
Copyright © 2009 The American Society for Pharmacology and Experimental Therapeutics
Mol Pharmacol 75:502–513, 2009

Vol. 75, No. 3
51607/3439302
Printed in U.S.A.

Evidence for a Direct and Functional Interaction between the Regulators of G Protein Signaling-2 and Phosphorylated C Terminus of Cholecystokinin-2 Receptor[S]

Ingrid Langer, Irina G. Tikhonova, Cyril Boulègue, Jean-Pierre Estève, Sébastien Vatinel, Audrey Ferrand, Luis Moroder, Patrick Robberecht, and Daniel Fourmy

Department of Biological Chemistry and Nutrition, Faculty of Medicine, Université Libre de Bruxelles, Brussels, Belgium (I.L., P.R.); Institut National de la Santé et de la Recherche Médicale, Unit 858, Toulouse, France (I.G.T., J.P.E., S.V., A.F., D.F.); Université de Toulouse 3, Toulouse, France (I.G.T., J.P.E., S.V., A.F., D.F.); and Max Planck Institut für Biochemie, Martinsried, Germany (C.B., L.M.).

Received August 29, 2008; accepted December 5, 2008

ABSTRACT

Signaling of G protein-coupled receptors (GPCRs) is regulated by different mechanisms. One of these involves regulators of G protein signaling (RGS), which are diverse and multifunctional proteins that bind to active Gα subunits of G proteins and act as GTPase-activating proteins. Little is known about the molecular mechanisms that govern the selective use of RGS proteins in living cells. We first demonstrated that CCK2R-mediated inositol phosphate production, known to be G_q-dependent, is more sensitive to RGS2 than to RGS4 and is insensitive to RGS8. Both basal and agonist-stimulated activities of the CCK2R are regulated by RGS2. By combining biochemical, functional, and in silico structural approaches, we demonstrate that a direct and functional interaction occurs between RGS2 and agonist-stimulated cholecystokinin receptor-2 (CCK2R) and identified the precise residues involved: phosphorylated Ser434 and Thr439 located in the C-terminal tail of CCK2R and Lys62, Lys63, and Gln67, located in the N-terminal domain of RGS2. These findings confirm previous reports that RGS proteins can interact with GPCRs to modulate their signaling and provide a molecular basis for RGS2 recognition by the CCK2R.

G protein-coupled receptors (GPCRs), also referred to as seven transmembrane domain receptors, represent the largest family of signal transducers for extracellular stimuli. Upon agonist binding, GPCRs undergo conformational changes allowing the interaction of cytoplasmic domains with heterotrimeric G proteins and promoting the exchange of GDP for GTP on the Gα subunit. This initiates the dissociation of the GTP-bound Gα subunit from the Gβγ heterodimer and the activation of downstream effector pathways. Signals are terminated after hydrolysis of Gα-bound GTP and reformation of the inactive trimeric complex (Pierce et al., 2002).

Many mechanisms that operate at the receptor or G protein level have evolved to fine-tune and regulate GPCR signaling. Among these, the most extensively studied is receptor desensitization/internalization, which contributes to rapid signaling fading even in the presence of continued agonist exposure. This process involves phosphorylation of receptors in the intracellular loops and/or carboxyl-terminal moiety, binding to β-arrestins, followed by binding to clathrin and adaptor protein AP2 (Reiter and Lefkowitz, 2006).

GPCR signaling can also be regulated by the regulators of G protein signaling (RGS), a family of diverse and multifunctional proteins that attenuate and/or modulate GPCR-mediated signaling in part by binding to active Gα subunits and by acting as GTPase-activating proteins (GAPs). RGS proteins family members share a conserved 120 amino acid domain, called the RGS box/domain, containing the binding site for Gα and responsible for the GAP activity. They differ in their amino- and carboxyl-terminal domains flanking the

This work was supported by the Association pour la Recherche contre le Cancer [Grant ARC 3756]; the Fonds National de la Recherche Scientifique, Belgium; and by Fondation pour la Recherche Medicale.
Article, publication date, and citation information can be found at http://molpharm.aspetjournals.org.
doi:10.1124/mol.108.051607.
[S] The online version of this article (available at http://molpharm.aspetjournals.org) contains supplemental material.

ABBREVIATIONS: GPCR, G protein-coupled receptor; RGS, regulator of G protein signaling; GAP, GTPase-activating protein; CCK, cholecystokinin; CCK2R, cholecystokinin-2 receptor; CCK9s, sulfated [Thr^{28},Nle^{31}]-CCK25–33; HA, hemagglutinin; DMEM, Dulbecco's modified Eagle's medium; PBS, phosphate-buffered saline; BSA, bovine serum albumin; IP, inositol phosphate; CHAPS, 3-[(3-cholamidopropyl)dimethylammonio]propanesulfonate; PAGE, polyacrylamide gel electrophoresis; GST, glutathione transferase.

RGS box that can contain structural domains and binding motifs for a variety of signaling proteins. RGS proteins are classified into six subfamilies based on the RGS box identities and common conserved regions outside the RGS box. The B/R4 subfamily (RGS1, -2, -4, -5, -8, -13, and -16) contains the simplest RGS proteins. Until very recently, they appeared to have no function other than modulating G protein activity (Hollinger and Hepler, 2002; Neubig and Siderovski, 2002). In this subfamily, RGS2 and RGS4 are so far the most studied. In particular, the role of exogenous and endogenous RGS2, as a biochemical regulator of levels of inositol trisphosphate and Ca^{2+} oscillation, was extensively investigated in permeabilized pancreatic acini from rat and from RGS2(−/−) mice, respectively (Luo et al., 2001; Wang et al., 2004). The in vivo function of RGS2 as an essential signaling molecule was shown in RGS2(−/−) mice presenting several abnormalities, including hypertension, prolonged vasoconstrictor signaling, and anxiety (Oliveira-Dos-Santos et al., 2000; Heximer et al., 2003).

The biochemical mechanisms of GAP activity and the structure of RGS proteins have been well characterized; however, little is known about the cellular mechanisms that regulate RGS proteins recruitment and use, although RGS proteins seem to regulate Gα functions through recognition of receptor in addition to their association with Gα (Zeng et al., 1998; Wang et al., 2002). Early evidence for RGS recognition by GPCR came from Xu et al. (1999), who reported that in pancreatic acinar cells, RGS1, -2, -4, and -16 displayed different regulatory potency toward $G_{q/11}$-dependent Ca^{2+} signaling in response to activation of three different GPCRs, the muscarinic cholinergic, bombesin, or cholecystokinin receptors. Since this early finding, a molecular mechanism for regulation of muscarinic receptor M1 by RGS2 involving a direct interaction was reported (Bernstein et al., 2004; see *Discussion*, below), but the precise explanation that different RGS display different potencies toward $G_{q/11}$-dependent Ca^{2+} signaling in response to activation of distinct receptors remains unknown.

Given our specific interest toward the cholecystokinin-2 receptor, we wanted to investigate the mechanism whereby signaling of this receptor is regulated by RGS proteins. The cholecystokinin (CCK)-2 receptor (CCK2R) belongs to family A of rhodopsin-like GPCRs. It binds both cholecystokinin and gastrin with a similar, high affinity (Dufresne et al., 2006). The CCK2R is expressed in the central nervous system and in the gut, where it represents the predominant CCK receptor subtype (Noble et al., 1999; Dufresne et al., 2006). CCK2R mediates a wide spectrum of CCK- and gastrin-induced biological effects, including anxiety, pain perception, and gastric acid secretion, as well as controlling growth and differentiation of the gastric mucosa.

In the work presented here, we provided experimental evidence that a direct high-affinity and functional interaction occurs between the human CCK2R and RGS2, and we identified the interacting residues in the C-terminal phosphorylated region of CCK2R and in the N-terminal moiety of RGS2.

Materials and Methods

Materials. Sulfated [Thr^{28},Nle^{31}]-CCK25–33 (CCK9s) was synthesized as described previously (Moroder et al., 1981). ^{125}I-Na (2000 Ci/mmol) was from GE Healthcare (Les Ulis, France). Sulfated [Thr^{28},Nle^{31}]-CCK25–33 was conjugated with Bolton-Hunter reagent, purified, and radioiodinated as described previously and is referred as ^{125}I-CCK9s (Fourmy et al., 1989).

Site-Directed Mutagenesis and Transfection of COS-7 Cells. All mutant receptor cDNAs were constructed by oligonucleotide-directed mutagenesis (Quik Change site-directed mutagenesis kit; Stratagene, Strasbourg, France) using the human CCK2R cDNAs with HA or Myc epitope tag at the amino terminus cloned into pRFENeo vector as template. Truncated receptors at the C terminus were obtained by introducing a stop codon (TGA) at position 410 (CCK2[1–409]), 430 (CCK2[1–429]), or 440 (CCK2[1–439]). The cDNA for mouse RGS2 with an HA epitope tag at the amino terminus subcloned into pCR3.1 was a gift from Luc De Vries (Institut de Recherche Pierre Fabre, Castres, France). The cDNA for human RGS4 and RGS8 with HA epitope TAG at the amino terminus subcloned into pcDNA3.1 was obtained from the UMR cDNA Resource Center (http://www.cdna.org). Truncated RGS2 at the N terminus were obtained by insertion of a BamHI restriction site followed by an initiating methionine at positions 24 to 26 (RGS2[28–211]), 51 to 53 (RGS2[54–211]), or 77 to 79 (RGS2[80–211]) by using oligonucleotide-directed mutagenesis. Modified plasmids were then digested by BamHI and XhoI restriction enzymes to allow excision of RGS2 sequences [28–211], [54–211], or [80–211] that were then subcloned into pCR3.1 vector. For these truncated RGS2 constructs, an HA epitope tag was then inserted at the C terminus by site-directed mutagenesis. The presence of the desired and the absence of undesired mutations were confirmed by automated sequencing of the complete sequence (Applied Biosystems, Foster City, CA).

Transfection of COS-7 Cells. COS-7 cells (1.5×10^6) were plated onto 10-cm culture dishes and grown in Dulbecco's modified Eagle's medium (DMEM) containing 5% fetal calf serum in a 5% CO_2 atmosphere at 37°C. After overnight incubation, cells were transfected with 0.5 μg/plate of pRFENeo vectors containing the cDNA for the wild-type or mutated CCK_2 receptors in absence or in presence of vectors containing the cDNA for the wild-type or mutated RGS, using a modified DEAE-dextran method as described previously (Foucaud et al., 2006). In each experiment the total amount of DNA/plate was adjusted to 2.5 μg with empty pCR3.1 or pcDNA3.1 plasmids. Cells were transferred to 24-well plates at a density of 2×10^4 (binding studies) or 15×10^4 (Ins-P assay) cells/well 24 h after transfection.

Receptor Binding Assay. Approximately 24 h after the transfer of transfected cells to 24-well plates, the cells were washed with phosphate-buffered saline (PBS), pH 7.4, containing 0.1% Bovine Serum Albumin (BSA) and then incubated for 60 min at 37°C in 0.3 ml of DMEM containing 0.1% BSA with 50 pM ^{125}I-CCK9s in the presence or in the absence of unlabeled CCK9s. The cells were washed twice with ice-cold PBS, pH 7.4, containing 2% BSA, and cell-associated radioligand was collected by cell lysis with 0.1 N NaOH. The radioactivity was directly counted in a γ-counter (AutoGamma; PerkinElmer Life and Analytical Sciences, Waltham MA). Receptor density (B_{max}) and dissociation constant (K_d) were calculated from homologous ^{125}I-CCK9s/CCK9s competition binding experiments using Ligand software (Kell, Cambridge, UK).

Inositol Phosphates Assay. Approximately 24 h after the transfer to 24-well plates and after overnight incubation in DMEM containing 2 μCi/ml [*myo*-2-^{3}H]inositol (GE Healthcare, Les Ulis, France), the transfected cells were washed with DMEM and then incubated for 30 min in 1 ml/well DMEM containing 20 mM LiCl at 37°C. The cells were washed with inositol phosphate (IP) buffer at pH 7.45: PBS containing 135 mM NaCl, 20 mM HEPES, 2 mM $CaCl_2$, 1.2 mM $MgSO_4$, 1 mM EGTA, 10 mM LiCl, 11.1 mM glucose, and 0.5% BSA. The cells were then incubated for 60 min at 37°C in 0.3 ml of IP buffer with or without increasing CCK9s concentration. The reaction was stopped by adding 1 ml of methanol/HCl to each well, and the content was transferred to a column (Dowex AG 1-X8, formate form; Bio-Rad Laboratories, Hercules, CA) for the determination of inositol phosphate. The columns were washed twice with 3

ml of distilled water and twice with 2 ml of 5 mM sodium tetraborate/60 mM sodium formate. The content of each column was eluted by addition of 2 ml of 1 M ammonium formate/100 mM formic acid. Radioactivity of 1 ml of the eluted fraction was evaluated using a liquid scintillation counter (PerkinElmer Life and Analytical Sciences). EC_{50} (potency), which corresponded to concentrations of CCK9s giving half-maximal stimulation, were calculated from dose-effect curves by nonlinear regression curve-fitting using Prism software (GraphPad Software, San Diego, CA). Maximal efficacy (E_{max}) corresponded to inositol phosphate production achieved in the presence of supramaximal concentrations of CCK.

Preparation of COS-7 Cell Lysate. Thirty-six to 48 h after transfection, cells were washed twice with PBS and once with buffer consisting of 50 mM HEPES, 150 mM NaCl, 10 mM EDTA, 10 mM $Na_4P_2O_7$, 100 mM NaF, and 2 mM orthovanadate, pH 7.5. Cells were then lysed after 30-min incubation on ice in the same buffer containing 1.5% CHAPS and Complete protease inhibitor cocktail (Roche Diagnostics, Indianapolis, IN). The remaining insoluble material was eliminated by centrifugation at 15,000*g* for 10 min at 4°C. Protein concentration was evaluated by using BCA assay kit (Pierce, Rockford, IL).

Western Blot. Protein samples were subjected to 12% SDS-polyacrylamide gel electrophoresis (PAGE) and then electroblotted to nitrocellulose membrane. Nitrocellulose membrane was incubated in blocking buffer (PBS + 3% nonfat dry milk + 0.1% Tween 20) for 1 h at room temperature then probed with mouse anti-HA antibody (Covance Research Products, Princeton, NJ) diluted 1:1000 in PBS + 1% milk + 0.1% Tween 20 overnight at 4°C. Membranes were washed three times in PBS + 0.1% Tween 20, then probed with horseradish peroxidase goat anti-mouse antibody (Pierce) diluted 1:50.000 in PBS + 0.1% Tween 20 for 1 h at room temperature. Proteins were visualized using SuperSignal West Pico Chemiluminescent Substrate (Pierce). To verify that the same amount of protein was loaded on the gel, the membranes were stripped and re-probed using a mouse anti-GAPDH antibody (Millipore Bioscience Research Reagents, Temecula, CA) diluted 1:5000.

Pull-Down Assay. Lysates of COS-7 cells expressing wild-type or mutated HA-CCK2R were mixed with 100 μg of biotinylated fragment of RGS2 (sequence 54–79) bound to 250 μl of Sepharose-streptavidin beads (GE Healthcare) and incubated by rotating overnight at 4°C. Beads were pelleted and washed 10 times with buffer containing 20 mM NaH_2PO_4 and 150 mM NaCl, pH 7.5, and bound proteins were eluted with SDS sample buffer. Samples were boiled for 5 min, centrifuged briefly to pellet beads, resolved on 9% SDS-PAGE and transferred to nitrocellulose membrane. Membrane was probed with mouse anti-HA antibody (Covance) diluted 1:1000 as described under *Western Blot*.

Immunoprecipitation and Determination of Receptor Phosphorylation Levels. Thirty-two h after transfection with HA-CCK2R constructs, COS-7 cells were cultured in phosphate-free DMEM for 16 h and then incubated for 2 h at 37°C in same medium containing 200 μCi of acid-free [^{32}P]orthophosphate (MP Biomedicals). At the end of this labeling period, CCK9s was added. After agonist exposure, cells were washed three times with ice-cold buffer consisting of 10 mM HEPES, 4.2 mM $NaHCO_3$, 11.7 mM glucose, 1.2 mM $MgSO_4$, 4.7 mM KCl, 118 mM NaCl, and 1.3 mM $CaCl_2$, pH 7.4, and then lysed as described under *Preparation of COS-7 Cell Lysate*. The cell lysate was added to 30 μl of a protein G-Sepharose suspension (GE Healthcare) previously coated during 30 min with 1 μl of mouse anti-HA antibody (Covance). After overnight incubation under light agitation at 4°C, the Sepharose beads were separated by centrifugation and washed five times with buffer consisting of 30 mM HEPES, 30 mM NaCl, and 1% Triton X-100, pH 7.5. The final bead pellet was resuspended in SDS sample buffer. After heating at 95°C for 5 min., the samples were resolved by SDS-PAGE using 9% gel. The gel was fixed and dried and the phosphorylated bands were detected and quantified by filmless autoradiographic analysis.

Purification of Recombinant RGS2 Proteins. RGS2 and RGS2[80–211] DNA sequences inserted into pCR3.1 vector were digested by BamHI and XhoI restriction enzymes and then subcloned into pET28a vector (Novagen, Madison, WI) for bacterial expression with a N-terminal hexa-histidine tag. RGS2 and RGS2[80–211] in pET28a were transformed into BL21(DE3) *Escherichia coli*. For each protein, 1 liter of culture was grown in Luria broth/kanamycin and induced with 1 mM isopropyl-β-D-thiogalactopyranoside for 2 h at 37°C. Bacteria were kept 5 min on ice then pelleted. The pellets were frozen at −80°C overnight and then resuspended in 25 ml of binding buffer (20 mM Na_2HPO_4, 0.5 M NaCl, 20 mM imidazole, and 1% Triton X-100, pH 7.4) supplemented with Complete protease inhibitor cocktail (Roche) and snap-frozen two times in liquid nitrogen. Bacteria were thawed, sonicated, kept on ice for 30 min followed by centrifugation at 15,000*g* at 4°C for 20 min to collect soluble materials. The supernatant was then incubated with 1.5 ml of nickel-equilibrated Chelating Sepharose Fast Flow (GE Healthcare) for 2 h at 4°C. After incubation, Sepharose beads were pelleted, washed three times with 7.5 ml of wash buffer (20 mM Na_2HPO_4, 0.5 M NaCl, 100 mM imidazole, and 1% Triton X-100, pH 7.4), and eluted with elution buffer (20 mM Na_2HPO_4, 0.5 M NaCl, 200 mM imidazole, pH 7.4). Proteins were then purified and concentrated by ultrafiltration using a 10-kDa cut-off membrane (Centricon; Millipore Corporation, Billerica, MA). Protein concentration was determined by Bradford reagent (Bio-Rad Laboratories) and was estimated to be 90% pure as determined by Coomassie blue staining of SDS-PAGE gel.

Purification of the CCK2 Receptor Third Intracellular Loop. The sequence corresponding to the third intracellular loop of the human CCK2 receptor (3il[244–335]) was subcloned into the bacterial expression vector pGEX-4T2 (GE Healthcare) with an N-terminal GST tag. *E. coli* BL21 strains were then transformed with this construct and grown in 500 ml of Luria broth/ampicillin medium. Protein production was induced by isopropyl-β-D-thiogalactopyranoside addition (1 mM) for 90 min at 30°C. After centrifugation, bacteria pellets were resuspended in a lysis buffer (10 mM Tris, 60 mM NaCl, 1 mM EDTA, 1% Triton X-100, and protease inhibitors), snap-frozen twice in liquid nitrogen, and sonicated. Lysates were then kept for 30 min at 37°C with 50 IU/ml DNase I, 2 mM dithiothreitol, 2.5 mM $MgCl_2$ and then centrifugated at 12,000 rpm for 30min. Supernatants were collected and incubated overnight with glutathione beads (Sigma-Aldrich, St. Louis, MO). The GST-3il[244–335] protein was eluted with 10 mM reduced glutathione. Proteins were purified and concentrated by ultrafiltration using a 10-kDa cut-off membrane, and their concentration was determined by Bradford reagent (Bio-Rad Laboratories). GST-3il[244–335] was estimated to be pure over 90% by Coomassie blue staining of SDS-PAGE gel.

Surface Plasmon Resonance Analysis. Surface plasmon resonance experiments were carried out on a BIA-core 3000 instrument (BIAcore AB, Uppsala, Sweden). The biotinylated peptides corresponding to C-terminal moiety of CCK2R: CCK2R[429–445], Biot-GGG-SIASLSRLSYTTISTLG; pS434T439, Biot-GGG-SIASLS-(*PO3*)RLSYTTISTLG; and pS434pT439, Biot-GGG-SIASLS(*PO3*)-RLSYT(*PO3*)TISTLG were synthesized on a Pioneer Peptide Synthesis System (Applied Biosystems) using the standard procedures of 9-fluorenylmethoxycarbonyl/*tert*-butyl chemistry on a Tentagel S Ram resin from Rapp polymere (Tübingen, Germany). Biotinylation was performed manually, and peptides were obtained after a 2-h treatment with trifluoroacetic acid/water/triisopropylsilane (95:2.5:2.5) or reagent B (trifluoroacetic acid/phenol/H_2O/triisopropylsilane 88:5:2.5:2.5). followed by precipitation in ice-cold methyl-*tert*-butyl-ether/hexane (2/1). All peptides were purified to high homogeneity (≥95%) by reversed-phase high-performance liquid chromatography, and their molecular weights were verified by electrospray ionization-mass spectrometry.

The biotinylated peptides were immobilized on chips with streptavidin-coated matrix (Chip SA BIAcore). GST-3il[244–335] was im-

mobilized on corboxymethylated dextran matrix (chip CM5 BIAcore) via standard EDC/NHS amine coupling (BIAcore). Different concentrations of hexahistidine-RGS2 and hexahistidine-RGS2[80–211] were passed over the immobilized peptides or GST-3il[244–335] protein, and kinetic and affinity constants were determined using BIAevaluation 4.0 software (BIAcore).

Molecular Modeling. The three-dimensional (3D) model of RGS2 in a water-lipid environment described previously (Tikhonova et al., 2006) was used for the investigation of RGS2 interactions with the C-terminal part of CCK2R (429–447 residues). The fully flexible docking of the C-terminal part of CCK2R in unphosphorylated/phosphorylated forms to RGS2 was done using Gold program (Jones et al., 1997). Each docking pose of the C-terminal part of CCK2R was evaluated by fitness scoring implemented in Gold and also visual

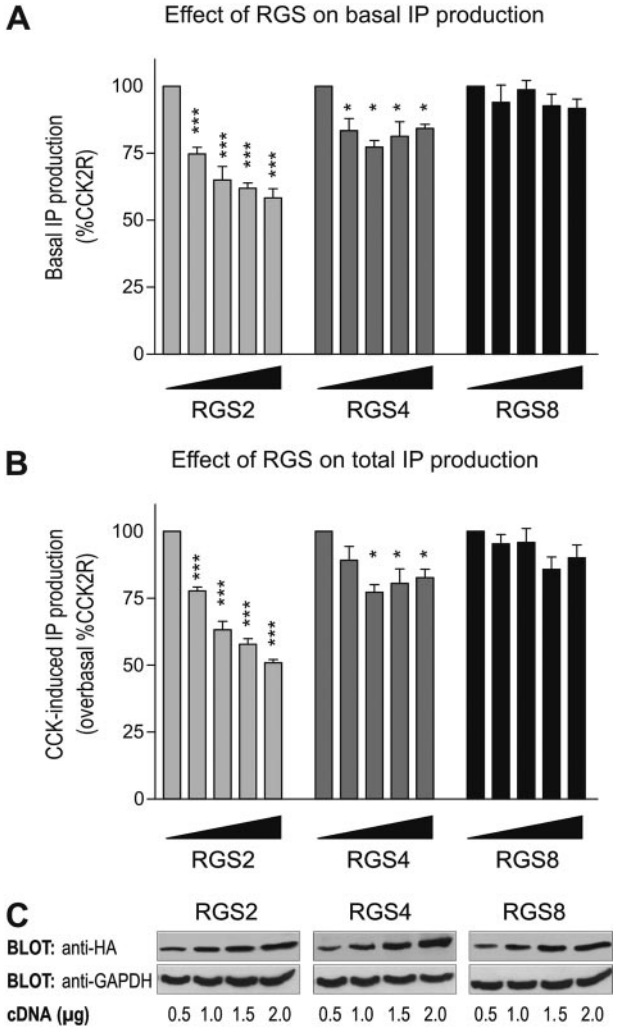

Fig. 1. Effect of coexpressing CCK2R and RGS proteins on CCK2R-mediated inositol phosphate production. Basal IP (A) and maximal IP production in response to 1 μM CCK9 evaluated in COS-7 cells cotransfected with CCK2R (0.5 μg) and increasing concentrations of RGS2, RGS4, and RGS8 (0.5–2 μg) (B). If necessary, total DNA quantity was adjusted to 2.5 μg with empty vector. Results represent the means ± S.E.M. of at least three independent experiments performed in duplicate. *, $p < 0.05$; ***, $p < 0.001$ determined by Mann-Whitney test. In all conditions, CCK potency was calculated from dose-effect curves (RGS2, EC_{50} = 0.53 ± 0.09 nM; RGS4, EC_{50} = 0.50 ± 0.05 nM; RGS8, EC_{50} 0.58 ± 0.06 nM) and CCK2R expression levels evaluated by binding studies (RGS2, 88.6 ± 9.7% of control, n = 10; RGS8, 102.9 ± 5.6% of control, n = 3; RGS4, 74.3 ± 8.5% of control, n = 4 $p < 0.05$; control values, B_{max_1} = 1.2 ± 0.1 and B_{max_2} = 2.3 ± 0.2 pmol/10^6 cells). C, Western Blot analysis of RGS protein expression levels. COS-7 cells coexpressing Myc-tagged CCK2R and HA-tagged RGS proteins were solubilized, resolved on 12% acrylamide-SDS gels, transferred to nitrocellulose membrane, and blotted with anti-HA antibody (top). The membranes were then stripped and re-probed using a mouse anti-GAPDH antibody (bottom). Representative of three independent experiments.

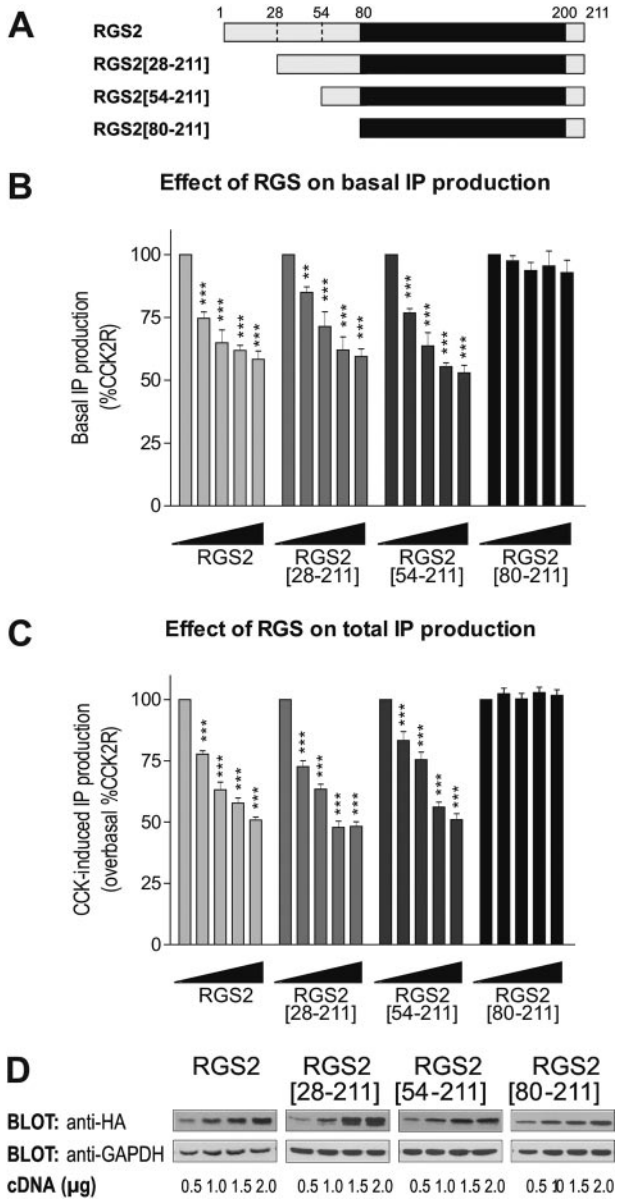

Fig. 2. Involvement of RGS2 N terminus in CCK2R-mediated signaling. A, schematic representation of the different RGS2 constructs tested. Basal IP (B) and maximal IP production in response to 1 μM CCK9 determined in COS-7 cells cotransfected with CCK2R (0.5 μg) and increasing concentrations of RGS2, RGS2[28–211], RGS2[54–211], and RGS2[80–211] (0.5–2 μg) (C). If necessary, total DNA quantity was adjusted to 2.5 μg with empty vector. Results represent the means ± S.E.M. of three independent experiments in duplicate. **, $p < 0.01$; ***, $p < 0.001$ determined by Mann-Whitney test. In all conditions, CCK potency was calculated from dose-effect curves (RGS2, EC_{50} = 0.53 ± 0.09 nM; RGS2[28–211], EC_{50} = 0.60 ± 0.06 nM; RGS2[54–211], EC_{50} = 0.51 ± 0.07 nM; RGS2[80–211], EC_{50} = 0.47 ± 0.06 nM) and CCK2R expression levels evaluated by binding studies (RGS2[28–211], 86 ± 10% of control, n = 3; RGS2[54–211], 92.1 ± 9.4% of control, n = 3; RGS2[80–211], 95.3 ± 6.3% of control, n = 3; control values, B_{max_1} = 1.2 ± 0.1 and B_{max_2} = 2.3 ± 0.2 pmol/10^6 cells). D, Western Blot analysis of RGS proteins expression levels. COS-7 cells coexpressing MYC-tagged CCK2R and wt or truncated HA-tagged RGS2 were solubilized, resolved on 12% acrylamide-SDS gels, transferred to nitrocellulose membranes, and blotted with anti-HA antibody (top). The membranes were then stripped and reprobed using a mouse anti-GAPDH antibody (bottom). Representative of three independent experiments.

inspection. The final complex of the C-terminal part of CCK2R and RGS2 was chosen based on the experimental validations. To investigate the stability of the interactions between RGS2 and the C-terminal part of CCK2R obtained from the docking studies, the final complex was submitted to 1-ns molecular dynamics simulation in water-lipid environment using Gromacs program (Van Der Spoel et al., 2005). For this purpose, we have used the coordinates of RGS2 and lipids that we obtained previously (Tikhonova et al., 2006), in which the C-terminal part was implemented, and the whole system was solvated and neutralized. The system was then minimized and submitted to molecular dynamics simulation. The protocol for the simulation was the same as described previously (Tikhonova et al., 2006). In brief, the simulation was performed at 310 K, the time step for integration was 2 fs, and the LINCS (linear constraint solver) algorithm was used to restrain bond lengths.

Results

RGS2 Modulates CCK2R-Mediated Inositol Phosphate Production. CCK2R is a G-protein-coupled receptor widely expressed in peripheral tissues and in the central nervous system. CCK2R-mediated biological effects result from a signaling cascade starting with G_q-dependent activation of phospholipase C (Dufresne et al., 2006; Marco et al., 2007). To identify potential RGS proteins involved in the modulation of CCK2R-mediated signaling, we expressed, in COS-7 cells, CCK2R in the absence or presence of increasing amounts of RGS2, RGS4 (both recognized regulators of G_q), or RGS8 (a regulator of $G_{i/o}$ and G_q). As shown in Fig. 1, basal (Fig. 1A) and CCK-induced (1 μM; Fig. 1B) inositol phosphate accumulation decreased in cells expressing RGS2 or RGS4 but not in those expressing RGS8. RGS2 effects were concentration-dependent, as shown by titration experiments with increasing amounts of transfected RGS coding plasmids (Fig. 1C). In all conditions, CCK potency and affinity were unaffected (data not shown). We next examined whether changes in the expression level of CCK2R could be at the origin of reduced signaling in the presence of increasing concentrations of RGS2 or RGS4. Regardless of the amount of RGS plasmid used, CCK2R expression levels were not significantly affected by coexpression of RGS2 or RGS8 but were slightly reduced in RGS4-expressing cells (see Fig. 1 legend). The reason for the slight decrease of CCK2R expression in RGS4-expressing cells is unknown. However, this first series

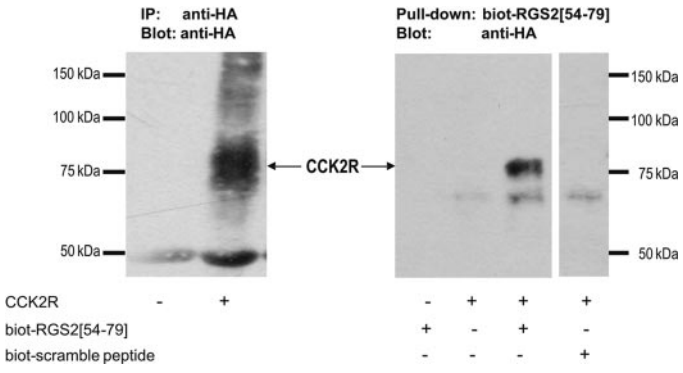

Fig. 3. Immunoprecipitation and pull-down assay of CCK2R. COS-7 cells were transfected or not with HA-tagged CCK2R and solubilized. Left, after immunoprecipitation with anti-HA antibody, proteins were blotted with anti-HA antibody. Right, COS-7 cell extracts were incubated with or without immobilized biotinylated peptide corresponding to the [54–79] sequence of RGS2 or biotinylated scramble peptide. Retained proteins were eluted and then blotted with anti-HA antibody.

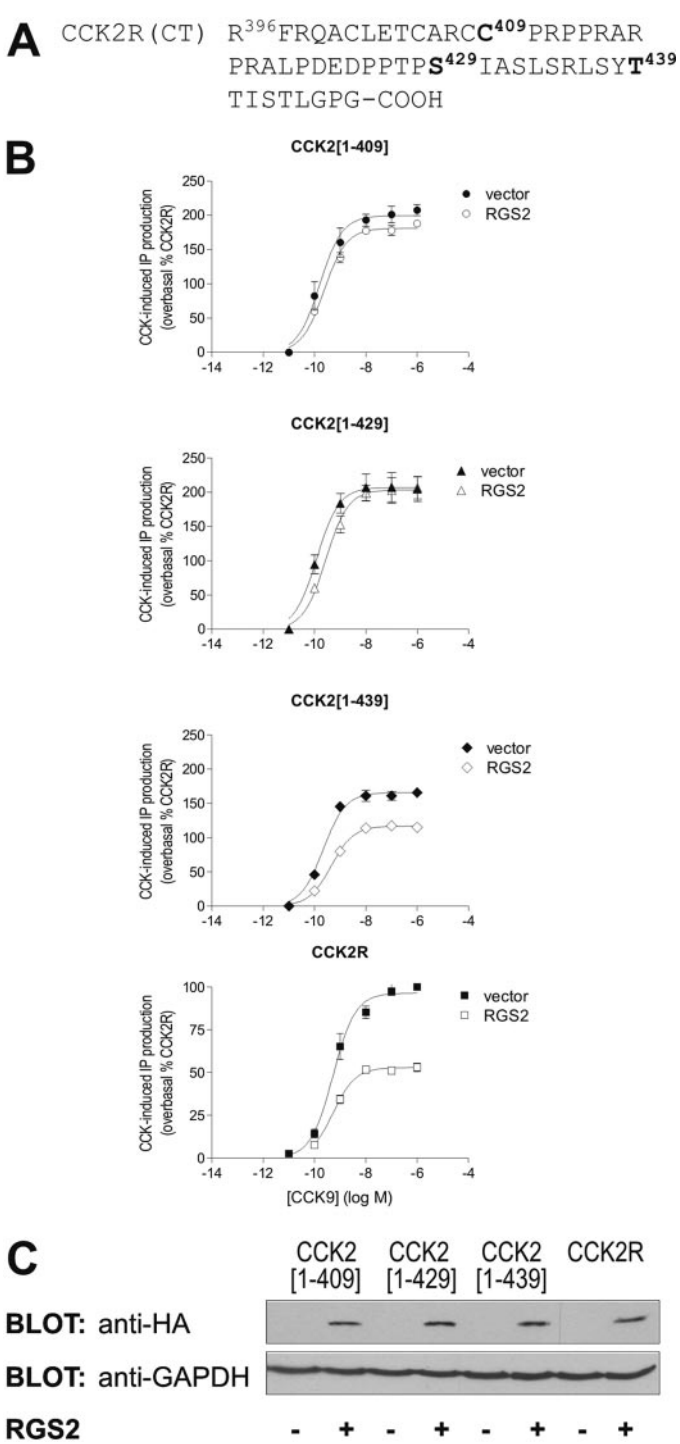

Fig. 4. Effect of coexpressing wild-type or truncated CCK2R and RGS2 on CCK9-induced inositol phosphate production. A, amino acid sequence of the C-terminal tail of the CCK2R. B, dose-effect curves of CCK9-induced inositol phosphate production of COS-7 cells transfected with 0.5 μg of wild-type (squares), CCK2[1–409] (circles), CCK2[1–429] (triangles), or CCK2[1–439] (diamonds) receptors in absence (closed symbols) or presence (open symbols) of 2 μg of RGS2. In the absence of RGS2, the total DNA quantity was adjusted to 2.5 μg with empty vector. Results represent the means ± S.E.M. of a minimum of three independent experiments in duplicate. C, Western Blot analysis of RGS2 expression levels. COS-7 cells expressing wt or truncated MYC-tagged CCK2R in the absence or presence of HA-tagged RGS2 were solubilized, resolved on 12% acrylamide-SDS gels, transferred to nitrocellulose membrane, and blotted with anti-HA antibody (top). The membranes were then stripped and re-probed using a mouse anti-GAPDH antibody (bottom). Representative of three independent experiments.

of data clearly supports that RGS2 is the most efficient regulator of both basal and CCK-stimulated CCK2R-mediated inositol phosphate production.

An Internal Sequence within the N-Terminal Domain of RGS2 Is Required for RGS2 Regulation of CCK2R-Mediated Inositol Phosphate Production. RGS2 is composed of an N-terminal region (RGS2[1–80] comprising an amphipathic helix), a central RGS box (RGS2[80–200], responsible for Gα subunit binding and GAP activity), and a short C-terminal domain (RGS2[201–211]; Kehrl and Sinnarajah, 2002). To determine whether a region other than the RGS box could be involved in the inhibitory effects of RGS2 on CCK2R-mediated inositol phosphate production, we evaluated the activity of truncated forms of RGS2 missing the first 27 (RGS2[28–211]), 53 (RGS2[54–211]), or 79 (RGS2[80–211]) N-terminal amino acids (Fig. 2A). Because wild-type CCK2R was previously demonstrated to exhibit a constitutive activity, leading to production of inositol phosphates in absence of agonist stimulation (Foucaud et al., 2006; Marco et al., 2007), effects of RGS2 and truncated variants were tested both on basal and CCK-stimulated production of inositol phosphates in cells. As shown in Fig. 2, RGS2[1–211], RGS2[28–211], and RGS2[54–211] were equally active on both basal (Fig. 2B) and CCK-induced (1 μM; Fig. 2C) inositol phosphate accumulation, whereas deletion of the entire N-terminal domain of RGS2 (RGS2[80–211]) completely abolished the RGS2 inhibitory effect. As with full-length RGS2, the inhibitory effect of active truncated RGS2 was concentration-dependent (Fig. 2D), and the exogenous coexpression of truncated RGS2 did not modify CCK potency and affinity or CCK2R expression levels (Fig. 2 legend). These results thus support that the RGS2 sequence [54–79] is required for RGS2 inhibition of CCK2R-mediated inositol phosphate production. This RGS2 sequence [54–79] has not yet been reported as critical for RGS2 activity. It is noteworthy that it comprises neither the amphipathic helix probably involved in RGS proteins recruitment to membrane nor the RGS box that comprises Gα subunit binding domain and GAP activity domain (Kehrl and Sinnarajah, 2002).

We further tested the hypothesis that sequence [54–79] of RGS2 may be physically involved in a functional complex including CCK2R. We carried out pull-down experiments using immobilized amino-biotinylated peptide corresponding to sequence 54 to 79 of RGS2 and solubilized from COS-7 cells expressing HA-CCK2R. We found that immobilized RGS2[54–79] fragment adsorbed a 80-kDa protein specifically revealed by an anti-HA antibody (Fig. 3). No specific protein band was observed after immobilization of irrelevant biotinylated peptide.

To evaluate whether the sequences identified are indeed involved in RGS2-CCK2R complex formation in a cellular context, we coexpressed HA-RGS2 constructs and MYC-CCK2R constructs in COS-7 cells and studied their cellular localization by immunofluorescence. When expressed alone in COS-7 cells, HA-RGS2, HA-RGS2[28–211], HA-RGS2[54–211], and HA-RGS2[80–211] localized in the cytoplasm and in the nucleus (Supplementary Data). After cotransfection with MYC-CCK2R, HA-RGS2 and HA-RGS2[28–211] primarily colocalized with the MYC-CCK2R at plasma membrane, HA-RGS2[54–211] colocalized in part with MYC-CCK2R at the plasma membrane, and RGS2[80–211] remained in intracellular compartments (supplementary data). All together, cellular studies with truncated RGS2 and pull-down experiments suggest that sequence [54–79] located in the N terminus of RGS2 is critical for the ability of RGS2 to modulate CCK2R mediated signaling and is potentially involved in a signaling complex including CCK2R.

A Sequence in the C-Terminal Tail of CCK2R Is Required for RGS2 Regulation of CCK2R-Mediated Inositol Phosphate Production. We next attempted to identify regions in CCK2R that are critical for RGS2 regulation of CCK2R-mediated signaling. We first considered the C-terminal tail of CCK2R as a candidate sequence as a result of frequent involvement of this region in GPCRs in multiple regulatory processes. Coexpression of RGS2 and CCK2R truncated in position 409 (CCK2[1–409]) or 429 (CCK2[1–429]) did not affect CCK-induced inositol phosphate production by the receptor mutants. However, the RGS2 inhibitory effect was partially restored for the CCK2[1–439] mutant, suggesting that a sequence between residues 429 and 439 was required for RGS2 inhibitory effect on inositol phosphate production (Fig. 4, Table 1). In contrast, the RGS2 inhibitory effect on basal inositol phosphate production was preserved for all truncated receptors tested (Table 1). We did not observe any changes in CCK affinity or receptor density (Table 1). Despite similar receptor densities, maximal inositol phosphate responses with truncated receptors were enhanced by approximately 2-fold compared with the wild-type CCK2R response. Basal inositol phosphate production was also enhanced by 1.5-fold with CCK2[1–409] (Fig. 5, Table 1). To determine whether the effect on truncated CCK2R seen in the absence of RGS2 was caused by the loss of interaction between RGS2 and CCK2R, we carried out pull-

TABLE 1

Summary of the effects of truncation of CCK2R on the affinity and biological activity of CCK either in the absence or presence of RGS2

Pharmacological study was performed on COS-7 cells transfected with wild-type or truncated CCK2R (0.5 μg) in absence or in presence of 2 μg of RGS2. IP production or binding parameters were determined as described under *Materials and Methods*. Results represent the means ± S.E.M. of at least three independent experiments performed in duplicate.

	Basal IP	CCK9s-Stimulated Ins-P		Binding Parameters			
		EC_{50}	E_{max}	K_{d_1}	K_{d_2}	B_{max_1}	B_{max_2}
	% CCK2R	*nM*	*% CCK2R*	*nM*		*pmol / 10^6 cells*	
CCK2R	100	0.53 ± 0.08	100	0.38 ± 0.04	3.0 ± 0.4	1.2 ± 0.1	2.3 ± 0.2
CCK2R + RGS2	58 ± 3	0.53 ± 0.09	52 ± 2	0.30 ± 0.04	3.2 ± 0.4	1.3 ± 0.1	2.2 ± 0.2
TR409	154 ± 7	0.16 ± 0.05	200 ± 8	0.45 ± 0.03	3.3 ± 0.4	1.3 ± 0.2	2.2 ± 0.1
TR409 + RGS2	63 ± 3	0.24 ± 0.05	182 ± 5	0.44 ± 0.06	2.3 ± 0.3	1.4 ± 0.2	1.9 ± 0.2
TR429	110 ± 4	0.12 ± 0.04	207 ± 8	0.42 ± 0.04	2.5 ± 0.3	1.2 ± 0.2	2.7 ± 0.4
TR429 + RGS2	64 ± 5	0.28 ± 0.08	204 ± 7	0.37 ± 0.05	2.4 ± 0.4	1.4 ± 0.2	2.4 ± 0.3
TR439	120 ± 7	0.22 ± 0.03	166 ± 3	0.45 ± 0.03	2.4 ± 0.3	1.1 ± 0.1	2.7 ± 0.4
TR439 + RGS2	68 ± 4	0.44 ± 0.05	117 ± 2	0.41 ± 0.03	2.3 ± 0.3	1.2 ± 0.1	2.3 ± 0.2

down experiments. As shown in Fig. 5, CCK2[1–439] but not CCK2[1–409] was adsorbed on the RGS2 fragment. All together, these results suggest that inhibitory action of RGS2 on CCK2R-mediated production of inositol phosphates after agonist stimulation occurs through formation of a functional complex comprising RGS2 and CCK2R and involving the sequence [54–79] in RGS2 and a sequence down-stream amino acid 429 in the CCK2R.

Evidence That Phosphorylated Ser434 and Thr439 Located in the C Terminus of CCK2R Are Critical for RGS2 Ability to Modulate CCK2R-Mediated Inositol Phosphate Production. We first examined the theoretical possibility of direct interaction between RGS2 and CCK2R by docking the C-terminal peptide (429–447 residues) of CCK2R to modeled RGS2. In our previous report (Tikhonova et al., 2006), we built the 3D model of the RGS2, including its N-terminal moiety, in several steps. Because the crystal of the RGS2 box was not available at the time of construction, we employed the crystal of the RGS4 box interacting with $G\alpha_{i1}$ protein (http://www.rcsb.org/; Protein Data Bank code 1AGR) to build the RGS2 box (Tikhonova et al., 2006) using homology modeling. Superimposition of our homology model of RGS2 with coordinates of RGS2 crystal subsequently released (Protein Data Bank code 2AF0) gives high degree of concordance. We then constructed separately the N-terminal region of RGS2 using the protein structure prediction server ROBETTA (http://www.robetta.net/) and data from circular dichroism spectroscopy analysis of RGS2 N-terminal fragment (39–79 residues) (Tikhonova et al., 2006). Finally, we assembled the N-terminal part of RGS2 to our model of the RGS2 box and optimized in a water-lipid environment for 5 ns to assess protein stability (details in Tikhonova et al., 2006). In the current work, to examine theoretical possibilities of a direct interaction between RGS2 and CCK2R, we attempted to dock the C-terminal peptide (429–447 residues) of CCK2R to this 3D model of RGS2. Although, during the docking, the C-terminal peptide was fully flexible, we could find no plausible contacts between the two proteins. We then considered that the C-terminal peptide of CCK2R containing a number of Ser and Thr residues represented potential sites of phosphorylation. These could be theoretically predicted using the NetPhos server (Blom et al., 1999). We therefore carried out a second docking experiment considering the C-terminal part phosphorylated either on Ser432, Ser434, Ser437, Tyr438, or Thr439. All obtained complexes showed energetically favorable contacts with positively charged residues Lys57, Lys62, and Lys63 of RGS2 (not shown).

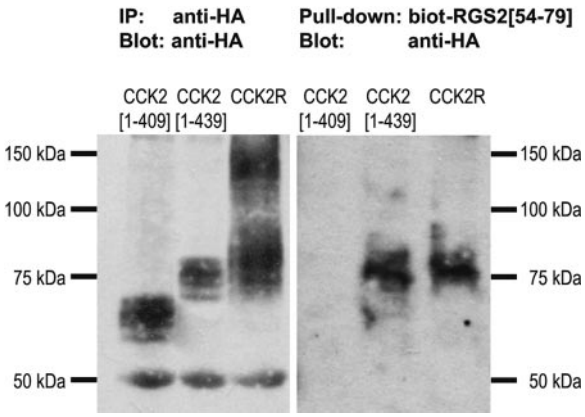

Fig. 5. Interaction of the N terminus of RGS2 with CCK2R constructs. COS-7 cells were transfected or not with wild-type or truncated HA-tagged CCK2R and solubilized. Left, after immunoprecipitation with anti-HA antibody, proteins were blotted with anti-HA antibody. Right, pull-down assay using immobilized biotinylated peptide corresponding to the sequence [54–79] of RGS2 followed by Western blot using anti-HA antibody of COS-7 cells expressing HA-tagged CCK2[1–409] (lane 1), CCK2[1–439] (lane 2), or wild-type (lane 3) CCK2R.

To evaluate the potential contribution of Ser432, Ser434, Ser437, Tyr438, and Thr439 located in the C terminus of CCK2R to the inhibitory effect of RGS2, we exchanged Ser/Thr residues for Ala and Tyr438 for Phe. For all mutants tested, the inhibitory effect of RGS2 on basal inositol phosphate production was preserved. In contrast, mutation of Ser434 or Thr439 to Ala reduced (S434A) or fully abolished (T439A, S434AT439A) the ability of RGS2 to modulate CCK-induced inositol phosphate accumulation (Fig. 6 and Table 2). CCK potency and affinity were similar to that observed for the wild-type receptor either in the absence or the presence of RGS2. Receptor binding assay indicated that all cell preparations expressed a similar receptor density (Table 2). We next evaluated the effect of mutations of Ser434 or Thr439 to glutamate, a residue known to mimic phosphorylated Ser/Thr residues. As shown in Table 2, the effect of RGS2 was restored in cells expressing S434E mutant but not T439E mutant.

Although well established for other GPCR, phosphorylation of CCK2R by GRK after repeated or sustained exposure to agonists has not yet been documented. We therefore investigated whether Ser434 and Thr439 were indeed phosphorylated after CCK exposure in living cells. As shown in Fig. 7A, CCK induced a rapid, dose-dependent stimulation of ^{32}P incorporation into a protein with an apparent molecular size of 85 kDa that was immunoprecipitated with the anti-HA antibody. The maximal signal was obtained after 5-min stimulation with 100 nM CCK. As shown in Fig. 7B, mutation of Ser434 and Thr439 to alanine (a nonphosphorylatable residue) led to 36 ± 8% reduction in CCK2R phosphorylation after normalization of the signal with receptor expression levels.

We further used plasmon resonance technology to experimentally verify in vitro whether a direct interaction between RGS2 and a phosphorylated C-terminal moiety of CCK2R can occur in the absence of any other cell proteins. We tested the binding to recombinant RGS2 of synthetic replicates of the C-terminal tail of CCK2R which were biotinylated on the N terminus and either phosphorylated or not on both Ser434 and Thr439 or phosphorylated only on Ser434. We observed a clear interaction between the immobilized CCK2R fragment doubly phosphorylated on Ser434 and Thr439 (pS434pT439) and RGS2, but no specific binding for the monophosphorylated CCK2R fragment (pS434T439) or the nonphosphorylated C-terminal of CCK2R used as a reference peptide to overcome nonspecific interactions between RGS2 and dextran carboxymethylated chips (Fig. 8A). Binding of RGS2 was dose-dependent (500 nM–8 μM) (Fig. 8B) and was completely abolished after removal of the N-terminal region of RGS2 (data not shown). Global fitting of these interactions resulted in an affinity constant of 79 ± 2 nM (calculated as the ratio between K_{off} and K_{on}) and a maximal binding of 600 ± 50 resonance units. We also tested the hypothesis that a direct interaction between the third intracellular loop of the CCK2R and RGS2 may occur. However, plasmon resonance

experiments could not detect any specific binding between recombinant RGS2 and a GST-fusion protein corresponding to the third intracellular loop of the CCK2R (GST-3il[244–335]) (data not shown). All together, these in silico and laboratory data strongly support the idea that regulation of CCK2R-mediated inositol phosphate production by RGS2 involves a direct interaction between the C-terminal phosphorylated of the human CCK2R and an internal sequence in the N-terminal region of RGS2.

Identification of Amino Acids within the N-Terminal Region of RGS2 That Participate to CCK2R Recognition. Starting with all available experimental results from the current study, the 3D model of the complex between RGS2 and C-terminal tail of CCK2R phosphorylated on Ser434 and Thr439 was chosen and optimized in a water-lipid environment. During simulation, stable contacts were achieved including ionic interactions involving phospho-Ser434 (pSer434) in CCK2R and Lys62 (RGS2), phospho-Thr439 (pThr439) in CCK2R and Lys63 (RGS2) as well as a hydrogen bond between pThr439 and Gln67 (RGS2) (Fig. 9). To further assess the molecular basis for specific recognition of RGS2, we first considered sequence alignment of the three RGS proteins tested in the current study. Alignment indicated that despite some homology, the N-terminal sequence of RGS8 differs from that of RGS2, especially at positions crucial for interaction. In contrast, RGS4 and RGS2 present strong homology in the loop of interest, except Gln67, which in the modeled complex (Fig. 9) interacts with pThr439 and is not present in RGS4. On this basis, we hypothesized that Gln67 may represent a key amino acid for specific recognition of CCK2R. We evaluated the effect of a mutation of Gln67 to Ala and found that the RGS2-Q67A mutant displayed 50% reduced efficacy in inhibiting CCK-induced inositol phosphate accumulation compared with bona fide RGS2 (data not shown). We then replaced the 59-to-67 sequence of RGS2 with the corresponding sequence of RGS4 (residues 36 to 45)

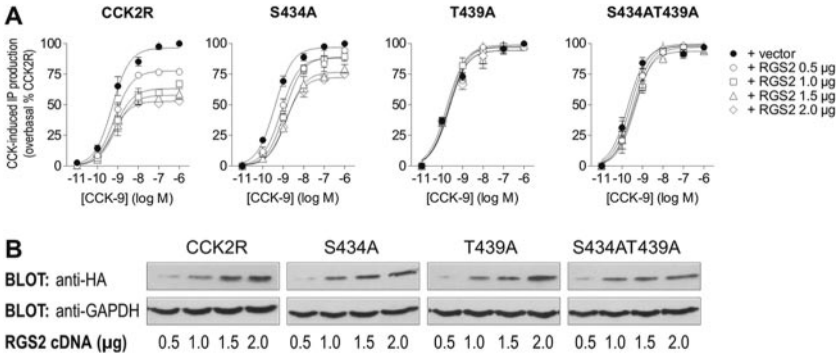

Fig. 6. Effect of Ser434 and Thr439 mutation of CCK2R on the inhibitory effect of RGS2. A, dose-effect curves of CCK9-induced inositol phosphate production of COS-7 cells transfected with 0.5 μg of wild-type or mutated CCK2R in the absence (closed symbols) or presence (open symbols) of increasing concentrations of RGS2 (0.5–2 μg). If necessary, total DNA quantity was adjusted to 2.5 μg with empty vector. Results represent the means ± S.E.M. of a minimum three independent experiments in duplicate. B, Western blot analysis of RGS2 expression levels. COS-7 cells coexpressing wt or mutated MYC-tagged CCK2R and HA-tagged RGS2 were solubilized, resolved on 12% acrylamide-SDS gels, transferred to nitrocellulose membranes, and blotted with anti-HA antibody (top). The membranes were then stripped and reprobed using a mouse anti-GAPDH antibody (bottom). Representative of three independent experiments.

TABLE 2

Summary of the effects of the mutation of CCK2R on the affinity and the biological activity of CCK either in the absence or presence of RGS2

Pharmacological study was performed on COS-7 cells transfected with wild-type or truncated CCK2R (0.5 μg) in absence or in presence of 2 μg of RGS2. Ins-P production or binding parameters were determined as described under *Materials and Methods*. Results represent the means ± S.E.M. of at least three independent experiments performed in duplicate.

	Basal IP	CCK9s-Stimulated IP		Binding Parameters			
		EC_{50}	E_{max}	K_{d_1}	K_{d_2}	B_{max_1}	B_{max_2}
	% CCK2R	*nM*	*% CCK2R*	*nM*		*pmol / 10^6 cells*	
CCK2R	100	0.53 ± 0.08	100	0.38 ± 0.04	3.0 ± 0.4	1.2 ± 0.1	2.3 ± 0.2
CCK2R + RGS2	58 ± 3	0.53 ± 0.09	52 ± 2	0.30 ± 0.04	3.2 ± 0.4	1.3 ± 0.1	2.2 ± 0.2
S432A	103 ± 4	0.51 ± 0.05	98 ± 3	0.40 ± 0.03	3.3 ± 0.4	1.3 ± 0.2	2.2 ± 0.2
S432A + RGS2	56 ± 4	0.62 ± 0.05	58 ± 2	0.44 ± 0.06	2.7 ± 0.3	1.4 ± 0.2	2.0 ± 0.2
S434A	98 ± 5	0.44 ± 0.04	95 ± 3	0.37 ± 0.04	2.8 ± 0.3	1.3 ± 0.2	2.4 ± 0.3
S434A + RGS2	**55 ± 5**	**0.45 ± 0.05**	**72 ± 2**	**0.36 ± 0.05**	**2.6 ± 0.4**	**1.2 ± 0.2**	**2.3 ± 0.3**
S437A	96 ± 6	0.61 ± 0.08	94 ± 3	0.45 ± 0.03	2.7 ± 0.3	1.2 ± 0.1	2.5 ± 0.4
S437A + RGS2	60 ± 4	0.59 ± 0.03	59 ± 3	0.41 ± 0.04	2.9 ± 0.4	1.3 ± 0.2	2.2 ± 0.2
Y438A	102 ± 5	0.55 ± 0.08	100 ± 2	0.44 ± 0.04	2.7 ± 0.3	1.4 ± 0.2	2.3 ± 0.2
Y438A + RGS2	53 ± 3	0.51 ± 0.09	57 ± 4	0.39 ± 0.04	2.8 ± 0.3	1.3 ± 0.2	2.2 ± 0.3
T439A	104 ± 4	0.48 ± 0.03	99 ± 3	0.40 ± 0.05	2.7 ± 0.4	1.2 ± 0.2	2.3 ± 0.3
T439A + RGS2	**60 ± 5**	**0.45 ± 0.05**	**97 ± 4**	**0.45 ± 0.03**	**3.0 ± 0.3**	**1.1 ± 0.3**	**2.2 ± 0.4**
S432AS437A	97 ± 5	0.61 ± 0.05	96 ± 2	0.42 ± 0.03	2.9 ± 0.4	1.3 ± 0.1	2.2 ± 0.2
S432AS437A + RGS2	56 ± 3	0.65 ± 0.08	56 ± 3	0.40 ± 0.04	3.2 ± 0.4	1.2 ± 0.1	2.1 ± 0.2
S434AT439A	101 ± 3	0.43 ± 0.05	97 ± 4	0.36 ± 0.03	3.1 ± 0.4	1.3 ± 0.2	2.2 ± 0.2
S434AT439A + RGS2	**59 ± 5**	**0.47 ± 0.06**	**100 ± 4**	**0.37 ± 0.05**	**2.9 ± 0.3**	**1.4 ± 0.2**	**2.1 ± 0.2**
S434E	99 ± 6	0.54 ± 0.05	98 ± 2	0.39 ± 0.04	3.1 ± 0.4	1.3 ± 0.2	2.2 ± 0.2
S434E + RGS2	**66 ± 4**	**0.58 ± 0.07**	**56 ± 2**	**0.40 ± 0.04**	**3.0 ± 0.4**	**1.2 ± 0.2**	**2.1 ± 0.2**
T439E	102 ± 5	0.49 ± 0.06	96 ± 3	0.38 ± 0.04	2.9 ± 0.5	1.3 ± 0.2	2.2 ± 0.2
T439E + RGS2	**62 ± 4**	**0.64 ± 0.07**	**91 ± 4**	**0.35 ± 0.05**	**2.8 ± 0.3**	**1.2 ± 0.1**	**2.3 ± 0.2**

and replaced the 36-to-45 sequence of RGS4 with the corresponding sequence of RGS2 (residues 59 to 64) and examined loss or gain of function of the chimeric RGS2/RGS4. The choice of the sequences replaced in chimeric RGS protein constructs was driven by 1) amino acids (Lys62, Lys63, and Gln67) identified by molecular modeling as interacting partners of phosphorylated Ser434 and Thr439 of CCK2R and 2) the presence of a proline (Pro59) upstream of Lys62, Lys63, and Gln67 in RGS2 that is not conserved in RGS4 and that may account for correct positioning and access of these amino acids. As shown in Fig. 10, the replacement of the PKTGKKSKQQ sequence in RGS2 by the corresponding sequence in RGS4 led to a loss of approximately 50% in the ability of RGS2 to reduce CCK-mediated inositol phosphate accumulation, whereas insertion of this RGS2 sequence in RGS4 significantly increased the inhibitory effect of RGS4, chimeric RGS4/2 being almost as effective as wild-type RGS2. As with the wild-type RGS proteins, coexpression of chimeric RGS proteins did not modify CCK potency (Fig. 10), affinity (data not shown), or CCK2R expression levels.

Discussion

G protein-coupled receptors represent one of the most important families of signaling proteins, with ubiquitous distribution throughout the animal and plant kingdoms. The understanding of their functioning and their regulatory mechanisms represents a continuous challenge. In this study, we first demonstrated that CCK2R-mediated inositol phosphate production, known to be G_q-dependent, is more sensitive to RGS2 than to RGS4 and insensitive to RGS8. Moreover, we showed that the N-terminal region of RGS2 contains a region located between residues 54 and 79 that is required for RGS protein activity on CCK2R signaling and for the formation of a complex with CCK2R. We were surprised to also find that the region of RGS2 between residues 54 and 79 modulates not only agonist-stimulated CCK2R-mediated signaling but also agonist-independent CCK2R-mediated signaling (basal activity or constitutive activity of the receptor), a phenomenon not already reported. These data are in line with those from other studies that reported the importance of the N-terminal region of RGS2 in regulation of GPCRs signaling. Indeed, deletion of this domain was shown to reduce the ability of RGS proteins to attenuate G_q-dependent signaling and eliminates receptor selectivity (Zeng et al., 1998; Bernstein et al., 2004; Hague et al., 2005). Moreover, N terminus of RGS proteins was reported to play

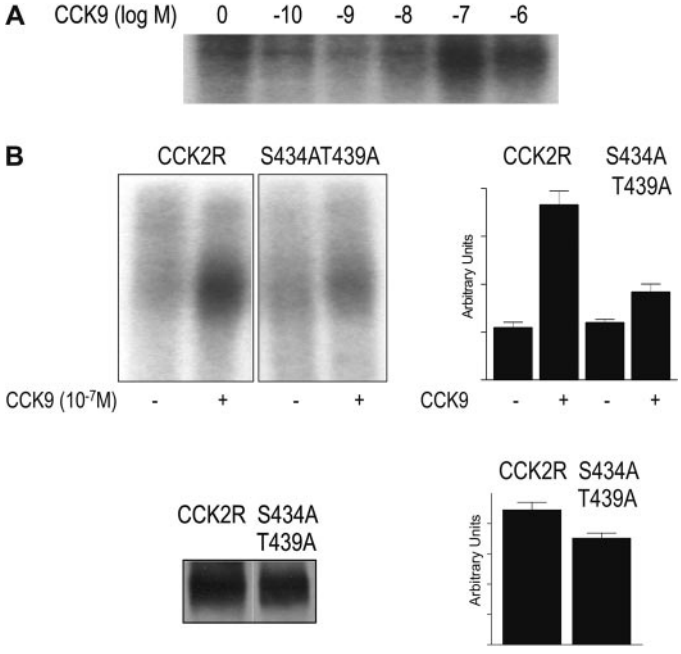

Fig. 7. CCK-induced phosphorylation of CCK2 receptor. Receptor phosphorylation levels were evaluated after preincubation of COS-7 cells with inorganic ^{32}P followed by CCK stimulation and receptor immunoprecipitation with anti-HA antibody. The labeled receptors were visualized by autoradiography after SDS page. A, dose-effect study after 5-min CCK stimulation. B, CCK2 and S434AT439A receptor phosphorylation levels after 5-min stimulation with 100 nM CCK (top). On the same cell preparation, relative receptor expression levels were evaluated by immunoprecipitation/Western Blot using anti-HA antibody (bottom) for signal normalization of phosphorylation. The two graphs on the right represent the integration of the bands in arbitrary units. Representative of three independent experiments.

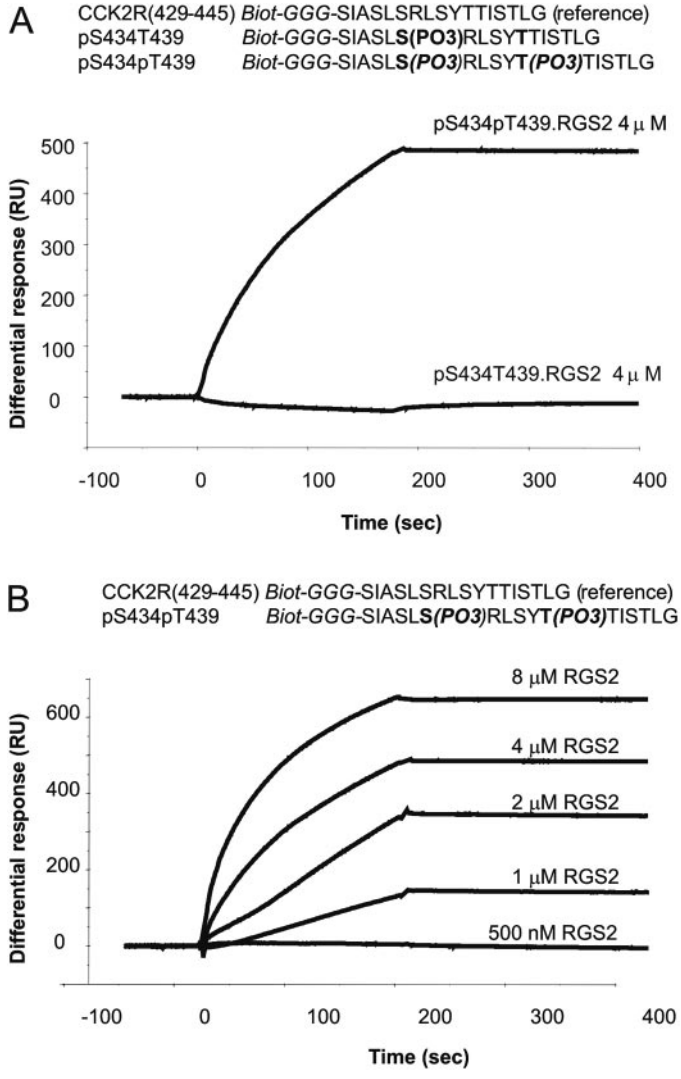

Fig. 8. Surface plasmon resonance analysis of CCK2R binding to RGS2. A, real-time interaction of doubly (pS434pT439) and mono-phosphorylated (pS434T439) C-terminal fragments of CCK2R to recombinant RGS2. B, dose-dependent binding of C-terminal doubly phosphorylated peptide (pS434pT439) to RGS2. Sensograms from the two experiments represent the differential response against nonphosphorylated C-terminal fragments of CCK2R used in the reference channel. This figure is representative of three separate experiments.

a role in the formation of a ternary complex made up of RGS-GPCR-scaffold protein or RGS-GPCR-G protein independent of agonist stimulation (Bernstein et al., 2004; Hague et al., 2005; Wang et al., 2005). On the other hand, three amino acids (Val9, Gln10, and His11) located in the N-terminal region of RGS2 were found to be crucial for binding and inhibition of type V adenylate cyclase activity (Salim et al., 2003). It is noteworthy that, between this adenylate cyclase binding region and the loop identified as being involved in CCK2R activity (this study), there is an amphipathic helix (residues 33 to 53) that was demonstrated to participate in the anchoring of RGS2 to the plasma membrane (Heximer et al., 2001). Our results showing that RGS2[54–211] lacking the amphipathic helix still inhibited CCK2R-mediated inositol phosphate production supports previous findings that RGS2 membrane targeting is not essential for RGS2 activity.

The current study also provides a set of converging experimental results indicating that two amino acids located in the C-terminal region of the CCK2R, namely Ser434 and Thr439, are crucial for the ability of RGS2 to modulate CCK-induced inositol phosphate production but not the basal response. It is noteworthy that these two amino acids must be phosphorylated for functional recognition of RGS2 after agonist stimulation. First, surface plasmon resonance experiments showed that a synthetic replicate of the C-terminal region of CCK2R that was phosphorylated on both Ser434 and Thr439 could bind directly with high affinity to recombinant RGS2 in the absence of any other protein. Second, immunoprecipitation of CCK2R after ^{32}P labeling showed that Ser434 and Thr439 were indeed phosphorylated after CCK exposure. In addition, replacement of Ser434 in the CCK2R by a Glu residue, known to mimic phosphorylated Ser/Thr, restored RGS2 regulation of CCK2R-dependent activity. Finally, molecular modeling provided structural support and likely physicochemical explanations for the direct interaction between RGS2 and CCK2R: the interaction between the RGS2 loop and the CCK2R fragment, phosphorylated on both Ser434 and Thr439, is energetically favorable; pSer434 forms an ionic interaction with K62 of RGS2 and pThr439 interacts with both Lys63 and Gln67 through ionic interaction and hydrogen bond, respectively (Fig. 9). Experimental results with the Q67A-RGS2 mutant and the RGS2/4 chimera displaying reduced ability to modulate CCK-induced

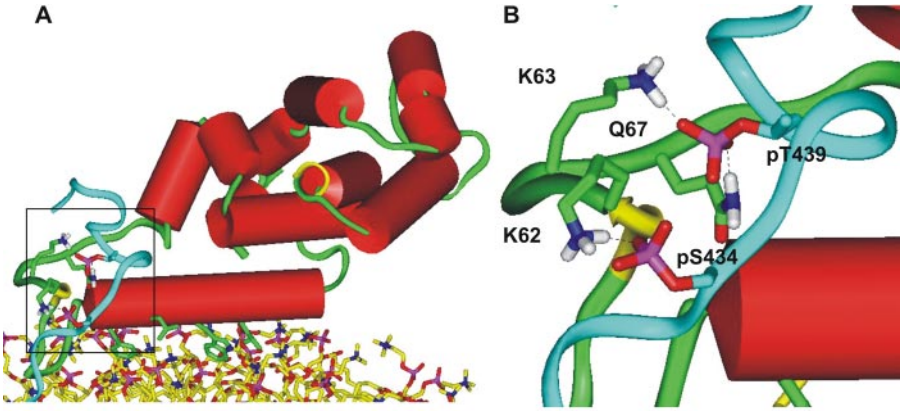

Fig. 9. Molecular model of [RGS2.CCK2R] interactions. A, results from docking of the C-terminal phosphorylated region of CCK2R to a modeled RGS2 interacting loop followed by a 5-ns molecular dynamics simulation. B, zoom view of the interacting regions. Helices in RGS2 are represented as red tubes. RGS2 loop and CCK2R C terminus are represented in green and blue ribbons, respectively. For clarity, only the carbon traces of side chains and interacting groups are depicted. Sequence alignment of RGS2 and RGS4 in the interacting region.

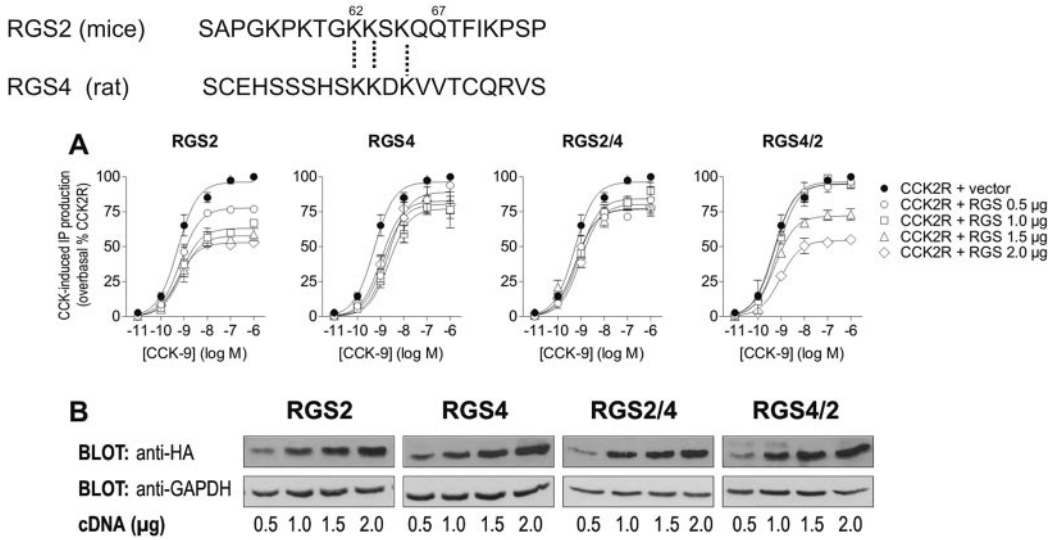

Fig. 10. Effect of RGS2 and RGS4 chimeric proteins on CCK-induced inositol phosphate production. A, dose-effect curves of CCK9-induced inositol phosphate production of COS-7 cells transfected with 0.5 μg of CCK2R in the absence (closed symbols) or presence (open symbols) of increasing concentrations of wt or chimeric RGS (0.5–2 μg). If necessary, total DNA quantity was adjusted to 2.5 μg with empty vector. Results represent the means ± S.E.M. of a minimum of three independent experiments in duplicate. In all conditions, CCK2R expression levels evaluated by binding studies (RGS2, 88.6 ± 9.7% of control, $n = 10$; RGS2/4, 85.9 ± 8.6% of control, $n = 3$; RGS4/2, 92.3 ± 7.5%; RGS4, 74.3 ± 8.5% of control, $n = 4$ $p < 0.05$). B, Western Blot analysis of RGS protein expression levels. COS-7 cells coexpressing MYC-tagged CCK2R and wt or chimeric HA-tagged RGS were solubilized, resolved on 12% acrylamide-SDS gels, transferred to nitrocellulose membranes, and blotted with anti-HA antibody (top). The membranes were then stripped and reprobed using a mouse anti-GAPDH antibody (bottom). Representative of three independent experiments.

inositol phosphate accumulation relative to intact RGS2, alongside those with the RGS4/2 chimera with equal efficiency to RGS2, not only confirm theoretical predictions but also provide a molecular basis for a higher efficacy of RGS2 compared with RGS4. This is probably due to Gln67, which is conserved in RGS2 among all species and is replaced by a valine in RGS4. The apparent discrepancy between results showing that Glu substitution of Thr439 did not restore RGS2 regulation of CCK2R-dependent activity and results from surface plasmon resonance showing that phosphorylation of both Thr439 and Ser434 is required for high-affinity binding of the synthetic replicate of the CCK2R C-terminal region to recombinant RGS2 can be explained by examining the contact region between RGS2 and the CCK2R in the modeled complex. Indeed, because of its composition and planar shape, the carboxylate function of Glu gives less opportunity of interaction and lower energy bonds relative to the phosphate moiety of Thr439, which presents one uncharged and three negatively charged oxygens distributed around the phosphor atom (Fig. 7). Precedents exist showing an inability of Glu substitution to mimic phosphorylated Thr, as in the 78-kDa protein kinase Mekk1, for example (Siow et al., 1997).

Several studies have recently addressed the mechanism whereby $G\alpha_q$-coupled receptors interact with preferred RGS with a high degree of specificity (Neitzel and Hepler, 2006). In fact, our current findings that a direct and functional interaction occurs between the RGS2 N-terminal and CCK2R C-terminal regions, but not the third intracellular loop, must be compared with available data with muscarinic M1, α_1-, β_2-adrenergic and μ-, δ-opioid receptors (Bernstein et al., 2004; Wang et al., 2005). RGS2 was shown to be recruited to the plasma membrane by the G_s-coupled β_2-adrenergic receptor and to bind to the third intracellular loop of the β_2-adrenergic receptor (Roy et al., 2006). Hague et al. (2005) demonstrated that the N terminus of RGS2 is required for association with α_{1A}-AR and selective inhibition of signaling and that three residues located in the third intracellular loop of α_{1A}-AR are essential for that interaction. On the other hand, Wang et al. (2005) found that another adrenergic receptor, the α_{1B}-AR, needs the scaffold protein spinophilin, which binds both the third intracellular loop of α_{1B}-AR and the N terminus of RGS2, to allow α_{1B}-AR.RGS2 association. In another study, RGS2, through its N-terminal moiety, was found to simultaneously bind to the M1 receptor third intracellular loop and activate G_q with its RGS domain (Bernstein et al., 2004). However, Bodenstein et al. (2007) were unable to provide functional evidence for RGS2 specificity at M1 versus M3 receptors but showed that differential proteasomal regulation of RGS protein level could represent an alternative mechanism controlling RGS proteins activity. It is also noteworthy that two studies performed on opioid receptors showed that morphine alters the selective association between μ-opioid receptors and specific RGS proteins (Garzon et al., 2005) and that RGS4 forms a stable complex with $G\alpha$, $G\beta\gamma$, and the C-terminal tail of both the μ- and the δ-opioid receptors but only after receptor activation (Georgoussi et al., 2006). These different data raise the possibility that recognition of RGS2 by GPCR, like that of $G\alpha$ subunit of trimeric G proteins, might occur through nonpredictable and differently located receptor sequences (Wess, 1997). Indeed, it is noteworthy that in the third intracellular loop of the mentioned receptors, no obvious consensus RGS proteins binding motifs could be identified. To explain the fact that N-terminal region of RGS2 interacts with and regulates effector proteins such as G-protein coupled receptor, adenylyl cyclase, tubulin, and the cation channel TRPV6, it has been proposed that that the N-terminal region of RGS2 comprises several short interaction motifs and/or can adopt distinct structures to bind various targets (Heximer and Blumer, 2007).

The fact that RGS2 regulation of activated CCK2R occurs through the phosphorylated C terminus of CCK2R leads us to propose a role for RGS2 in CCK2R desensitization complementary to that of β-arrestin. Indeed, the current paradigm for GPCR regulation is that, in addition to G protein coupling, GPCR activation by agonists also initiates the process of receptor desensitization, an adaptive response used by cells to stop G protein signaling (Pierce et al., 2002; Reiter and Lefkowitz, 2006). In many cases, agonist-specific receptor desensitization involves the following general mechanism: after binding of an agonist, GPCR undergoes conformational changes that allow it to bind to kinases (GPCR Ser/Thr kinases or GRK) and thereby become phosphorylated in intracellular loops and the carboxyl terminus. Phosphorylation of the receptor promotes the high-affinity binding of arrestins to the receptor, which both physically interdicts further coupling of G protein and may act as a signal transducer (Reiter and Lefkowitz, 2006). The binding of RGS2 (which enhances GTP hydrolysis rate leading to G protein uncoupling) to phosphorylated CCK2R could be an alternative/additional way of receptor desensitization to the steric hindrance of G protein coupling by β-arrestin. How this concept could be extended to other GPCRs remains to be studied. Moreover, the question of how RGS2, which is apparently associated to CCK2R in its basal state through a region different from the CCK2R C-terminal moiety, binds to the phosphorylated CCK2R C-terminal tail under agonist stimulation remains to be elucidated.

In conclusion, this study provides a set of converging results indicating that RGS2 binds directly to CCK2R to modulate its activity. It also allows the identification of the interacting sequences involved both at the CCK2R and the RGS2 level in conditions of agonist stimulation.

Acknowledgments

We sincerely thank Le Centre Informatique National de l'Enseignement Supérieur (Montpellier, France) for software and hardware support.

References

Bernstein LS, Ramineni S, Hague C, Cladman W, Chidiac P, Levey AI, and Hepler JR (2004) RGS2 binds directly and selectively to the M1 muscarinic acetylcholine receptor third intracellular loop to modulate $G_{q/11}$alpha signaling. *J Biol Chem* **279:**21248–21256.

Blom N, Gammeltoft S, and Brunak S (1999) Sequence and structure-based prediction of eukaryotic protein phosphorylation sites. *J Mol Biol* **294:**1351–1362.

Bodenstein J, Sunahara RK, and Neubig RR (2007) N-terminal residues control proteasomal degradation of RGS2, RGS4, and RGS5 in human embryonic kidney 293 cells. *Mol Pharmacol* **71:**1040–1050.

Dufresne M, Seva C, and Fourmy D (2006) Cholecystokinin and gastrin receptors. *Physiol Rev* **86:**805–847.

Foucaud M, Tikhonova IG, Langer I, Escrieut C, Dufresne M, Seva C, Maigret B, and Fourmy D (2006) Partial agonism, neutral antagonism, and inverse agonism at the human wild-type and constitutively active cholecystokinin-2 receptors. *Mol Pharmacol* **69:**680–690.

Fourmy D, Lopez P, Poirot S, Jimenez J, Dufresne M, Moroder L, Powers SP, and Vaysse N (1989) A new probe for affinity labelling pancreatic cholecystokinin receptor with minor modification of its structure. *Eur J Biochem* **185:**397–403.

Garzón J, Rodríguez-Muñoz M, and Sánchez-Blázquez P (2005) Morphine alters the

selective association between mu-opioid receptors and specific RGS proteins in mouse periaqueductal gray matter. *Neuropharmacology* **48:**853–868.
Georgoussi Z, Leontiadis L, Mazarakou G, Merkouris M, Hyde K, and Hamm H (2006) Selective interactions between G protein subunits and RGS4 with the C-terminal domains of the mu- and delta-opioid receptors regulate opioid receptor signaling. *Cell Signal* **18:**771–782.
Hague C, Bernstein LS, Ramineni S, Chen Z, Minneman KP, and Hepler JR (2005) Selective inhibition of alpha1A-adrenergic receptor signaling by RGS2 association with the receptor third intracellular loop. *J Biol Chem* **280:**27289–27295.
Heximer SP and Blumer KJ (2007) RGS proteins: Swiss army knives in seven-transmembrane domain receptor signaling networks. *Sci STKE* **2007:**pe2.
Heximer SP, Knutsen RH, Sun X, Kaltenbronn KM, Rhee MH, Peng N, Oliveira-dos-Santos A, Penninger JM, Muslin AJ, Steinberg TH, et al. (2003) Hypertension and prolonged vasoconstrictor signaling in RGS2-deficient mice. *J Clin Invest* **111:**445–452.
Heximer SP, Lim H, Bernard JL, and Blumer KJ (2001) Mechanisms governing subcellular localization and function of human RGS2. *J Biol Chem* **276:**14195–14203.
Hollinger S and Hepler JR (2002) Cellular regulation of RGS proteins: modulators and integrators of G protein signaling. *Pharmacol Rev* **54:**527–559.
Jones G, Willett P, Glen RC, Leach AR, and Taylor R (1997) Development and validation of a genetic algorithm for flexible docking. *J Mol Biol* **267:**727–748.
Kehrl JH and Sinnarajah S (2002) RGS2: a multifunctional regulator of G-protein signaling. *Int J Biochem Cell Biol* **34:**432–438.
Luo X, Popov S, Bera AK, Wilkie TM, and Muallem S (2001) RGS proteins provide biochemical control of agonist-evoked $[Ca^{2+}]_i$ oscillations. *Mol Cell* **7:**651–660.
Marco E, Foucaud M, Langer I, Escrieut C, Tikhonova IG, and Fourmy D (2007) Mechanism of activation of a G protein-coupled receptor, the human cholecystokinin-2 receptor. *J Biol Chem* **282:**28779–28790.
Moroder L, Wilschowitz L, Gemeiner M, Göhring W, Knof S, Scharf R, Thamm P, Gardner JD, Solomon TE, and Wünsch E (1981) [Cholecystokinin-pancreozymin synthesis. Synthesis of [28-threonine,31-norleucine]- and [28-threonine,31-leucine]cholecystokinin-pancreozymin-(25–33)-nonapeptide]. *Hoppe Seylers Z Physiol Chem* **362:**929–942.
Neitzel KL and Hepler JR (2006) Cellular mechanisms that determine selective RGS protein regulation of G protein-coupled receptor signaling. *Semin Cell Dev Biol* **17:**383–389.
Neubig RR and Siderovski DP (2002) Regulators of G-protein signalling as new central nervous system drug targets. *Nat Rev Drug Discov* **1:**187–197.
Noble F, Wank SA, Crawley JN, Bradwejn J, Seroogy KB, Hamon M, and Roques BP (1999) International Union of Pharmacology. XXI. Structure, distribution, and functions of cholecystokinin receptors. *Pharmacol Rev* **51:**745–781.
Oliveira-Dos-Santos AJ, Matsumoto G, Snow BE, Bai D, Houston FP, Whishaw IQ, Mariathasan S, Sasaki T, Wakeham A, Ohashi PS, et al. (2000) Regulation of T cell activation, anxiety, and male aggression by RGS2. *Proc Natl Acad Sci U S A* **97:**12272–12277.
Pierce KL, Premont RT, and Lefkowitz RJ (2002) Seven-transmembrane receptors. *Nat Rev Mol Cell Biol* **3:**639–650.
Reiter E and Lefkowitz RJ (2006) GRKs and beta-arrestins: roles in receptor silencing, trafficking and signaling. *Trends Endocrinol Metab* **17:**159–165.
Roy AA, Baragli A, Bernstein LS, Hepler JR, Hébert TE, and Chidiac P (2006) RGS2 interacts with Gs and adenylyl cyclase in living cells. *Cell Signal* **18:**336–348.
Salim S, Sinnarajah S, Kehrl JH, and Dessauer CW (2003) Identification of RGS2 and type V adenylyl cyclase interaction sites. *J Biol Chem* **278**(18)**:**15842–15849, 2003.
Siow YL, Kalmar GB, Sanghera JS, Tai G, Oh SS, and Pelech SL (1997) Identification of two essential phosphorylated threonine residues in the catalytic domain of Mekk1. Indirect activation by Pak3 and protein kinase C. *J Biol Chem* **272:**7586–7594.
Tikhonova IG, Boulègue C, Langer I, and Fourmy D (2006) Modeled structure of the whole regulator G-protein signaling-2. *Biochem Biophys Res Commun* **341:**715–720.
Van Der Spoel D, Lindahl E, Hess B, Groenhof G, Mark AE, and Berendsen HJ (2005) GROMACS: Fast, flexible, and free. *J Comput Chem* **26:**1701–1718.
Wang Q, Liu M, Mullah B, Siderovski DP, and Neubig RR (2002) Receptor-selective effects of endogenous RGS3 and RGS5 to regulate mitogen-activated protein kinase activation in rat vascular smooth muscle cells. *J Biol Chem* **277:**24949–24958.
Wang X, Huang G, Luo X, Penninger JM, and Muallem S (2004) Role of regulator of G protein signaling 2 (RGS2) in Ca^{2+} oscillations and adaptation of Ca^{2+} signaling to reduce excitability of $RGS2^{-/-}$ cells. *J Biol Chem* **279:**41642–41649.
Wang X, Zeng W, Soyombo AA, Tang W, Ross EM, Barnes AP, Milgram SL, Penninger JM, Allen PB, Greengard P, et al. (2005) Spinophilin regulates Ca^{2+} signalling by binding the N-terminal domain of RGS2 and the third intracellular loop of G-protein-coupled receptors. *Nat Cell Biol* **7:**405–411.
Wess J (1997) G-protein-coupled receptors: molecular mechanisms involved in receptor activation and selectivity of G-protein recognition. *FASEB J* **11:**346–354.
Xu X, Zeng W, Popov S, Berman DM, Davignon I, Yu K, Yowe D, Offermanns S, Muallem S, and Wilkie TM (1999) RGS proteins determine signaling specificity of G_q-coupled receptors. *J Biol Chem* **274:**3549–3556.
Zeng W, Xu X, Popov S, Mukhopadhyay S, Chidiac P, Swistok J, Danho W, Yagaloff KA, Fisher SL, Ross EM, et al. (1998) The N-terminal domain of RGS4 confers receptor-selective inhibition of G protein signaling. *J Biol Chem* **273:**34687–34690.

Address correspondence to: Daniel Fourmy, IFR 31, Institut Louis Bugnard, BP 84225, Unité INSERM U858–I2MR, 31432 Toulouse Cedex 4 France. E-mail: fourmyd@toulouse.inserm.fr